On the Splashing Threshold of a Single Droplet Impacting onto Rough and Porous Surfaces

A. Gipperich*, A. N. Lembach, I. V. Roisman and C. Tropea
Institute of Fluid Mechanics and Aerodynamics, Center of Smart Interfaces
Technische Universität Darmstadt Petersenstr. 32, 64287 Darmstadt, Germany

Abstract

Drop impact onto rough and porous surfaces is found in manifold applications such as ink jet printing and irrigation. An experimental work is carried out in order to classify different splashing outcomes of water and isopropanol droplets impacting onto various structured and unstructured rough and porous surfaces. The roughness of the surfaces is characterized with internationally standardized horizontal and vertical statistical roughness parameters. An empirical relationship is developed to describe the splashing threshold on rough surfaces. Further differences in the splashing threshold of porous surfaces are presented.

Introduction

Numerous industrial applications show the importance of drop impact onto solid surfaces. They include irrigation and pesticide spraying in agriculture, rain impacting on weather proof clothing, ink jet printing, high speed impact of water droplets in the last stages of steam turbines, and many other technological processes.

Drop impact onto solid surfaces is studied since the late 19th century [1]. A classification of different impact outcomes is given in [2]. After the droplet hits the surface a thin liquid lamella starts to propagate along the surface. Depending on roughness of the surface, the liquid properties, drop diameter and impact velocity the advancing lamella may be disturbed leading to fragmentation of the droplet in some cases, denoted as splash. The splashing threshold, above which the drop splashes, is described as a combination of the Reynolds and Weber numbers. One of the most known splash parameters is the K_S number ($K_S = We_S^{1/2} Re_S^{1/4}$, [6]). Detailed studies on the effects of liquid properties, such as surface tension and viscosity are given in [3, 5] and where an alternative splash parameter is proposed.

The influence of surface roughness on splash thresold is addressed in [7, 8, 2]. So far often the average roughness R_a is scaled by the drop diameter before impact D. Empirical equations to describe the splashing threshold, depending on R_a/D, were proposed by [7, 9]. The threshold of [7] depends also on the target material. The physics of such additional influence is not immediately clear.

No investigation on the splashing threshold of porous surfaces has been conducted up to date. The presented paper compares the splashing threshold of rough and porous targets. While R_a/D parameter as well as the K_S parameter were found to describe splashing in this study insufficiently a new measure of roughness slope to describe the splashing threshold is introduced.

Materials and Methods

Drop impact has been studied experimentally using a high-speed video system. A schematic view of the setup is depicted in Figure 1. A syringe equipped with a commercial needle was used to produce a single droplet. After the drop detaches from the needle tip it is accelerated by gravity, passes a light barrier to trigger the high speed camera, and impacts onto a target. By varying the drop height different impact velocities were achieved and thereby the splashing threshold on different target surfaces determined. Two different liquids were used to vary the surface tension: distilled water and isopropanol. The corresponding drop sizes are $D_{H_2O} = 2.4$ mm and $D_{iso} = 1.7$ mm, respectively. Liquid properties and impact parameters are summarized in Table 1. Droplet diameter D and impact velocity U of the droplet were measured from the images just prior to their contact with the targets surface.

Six different target materials were used within the experiments: bronze, stainless steel, polyethylene (PE), polytetrafluorethylene (PTFE), glass and ceramic. The porous structure of all the substrates is the result of sintering process. Figure 2 shows two examples of surface topography of a bronze and a PTFE target. Roughness of the porous targets within this study is irregular in all cases. This is also true for a number of impermeable targets, denoted as rough targets in the following. Several bronze and stainless steel targets were manufactured by face turning to achieve larger roughness values. These targets have a regular groove structure.

*Corresponding author: a_gipperich@gmx.de

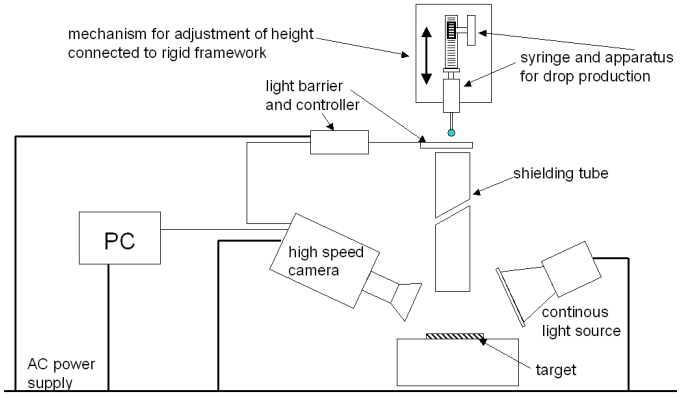

Figure 1. Schematic representation of the experimental setup.

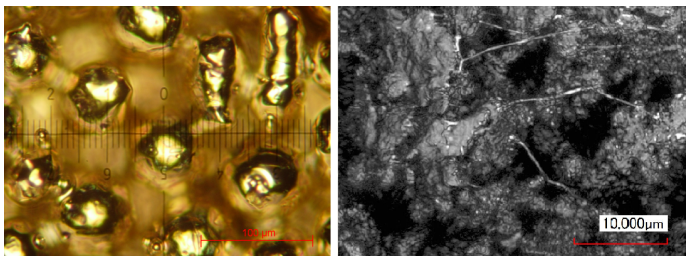

Figure 2. Left: surface structure of a porous bronze sample (porosity $\Phi \approx 30\%$; average pore diameter $d_{pore} \approx 12$ μm). Right: surface structure of a porous PTFE sample (porosity $\Phi \approx 43\%$; average pore diameter $d_{pore} \approx 20$ μm).

Several authors point out that the average roughness R_a is not sufficient to describe the splashing threshold on a rough surface (see e.g. [7, 2]). [2] are the first who additionally introduce a roughness wavelength as horizontal roughness measure for structured surfaces. In this study the roughness is characterized by two parameters namely the maximum height of the profile R_z (DIN EN ISO 4287) and the standardized number of peaks RP_c (EN 10049). Thereby a horizontal (RP_c) and a vertical (R_z) measure of the roughness elements is included into the analysis. All roughness parameters were measured according to DIN EN ISO 4288 by a tactile method, which showed more reliable results compared to confocal white light microscopy in case of porous samples with high porosity and large pore size. The primary profile was filtered to DIN EN ISO 11562(M1) and roughness values calculated according to the corresponding standard.

Porosity Φ and average pore diameter d_{pore} are varied to investigate their effect onto the splashing threshold. The total range of variation for the rough and porous targets, respectively, is summarized in Table 2.

Results and Discussion

Classification of Splashing Outcomes

Instability of drop spreading is enhanced by increasing impact velocity and surface roughness. The splashing threshold is characterized by the smallest impact velocity U_S and the drop diameter before impact D. A Weber number for the splashing threshold is defined by $We_S = (\rho D U_S^2)/\sigma$ with liquid density ρ and surface tension σ. While for $We < We_S$ the expanding liquid lamella can follow all surface perturbations without being splash, the lamella breaks up into a large number of fragments during its advance for values of $We > We_S$. Different mechanisms can lead to fragmentation of the lamella after impact. In the following a classification of different splashing outcomes will be given.

Figure 3 shows a sequence of images of a distilled water droplet splashing during the lamella advance on a rough unstructured polyethylene surface. The lamella is significantly disturbed by the roughness. Instabilities develop in form of fingers when the lamella expands. In the last image of the sequence it can be clearly seen that these fingers detach from the surface and break up into a large number of secondary droplets. Observations of the splashing on porous targets reveals a similar breakup of the lamella as shown in Figure 3.

Figure 4 shows two sequences of drop impact onto structured bronze surfaces. Impact velocity $U = 4.3\,m/s$

Liquid	μ [mPa · s]	σ [mN/m]	$\rho \cdot 10^3$ [kg/m^3]	U [m/s]	D [mm]	Θ_{adv} [°]
dist. water	1.00	72.5	1.00	$0.46 - 5.13$	2.4	19-133.3
isopropanol	2.27	23.0	0.78	$0.79 - 2.74$	1.7	-

Table 1. Properties of the liquids (viscosity μ, surface tension σ, density ρ) and the corresponding range of impact velocities U, drop diameters D. The advancing static contact angle Θ_{adv} has been measured on a smooth surface of each material.

Target material	$R_z\,[\mu m]$	$RP_c\,[peaks/cm]$	$\Phi\,[\%]$	$d_{pore}\,[\mu m]$
Bronze porous / rough	$25 - 65$ / $22 - 41$	$63 - 100$ / $84 - 33$	$25 - 31$ / –	$5 - 12$ / –
Ceramic porous / rough	$3 - 113$ / $7 - 276$	$32 - 152$ / $8 - 29$	$19 - 65$ / –	$< 5 - 30$ / –
Glass porous / rough	63 / $3 - 49$	70 / $55 - 207$	42 / –	$10 - 16$ / –
PE porous / rough	135 / $9 - 226$	39 / $18 - 110$	$44 - 52$ / –	$20 - 60$ / –
PTFE porous / rough	$31 - 136$ / $5 - 90$	$27 - 56$ / $24 - 110$	$40 - 45$ / –	$15 - 24$ / –
Stainless Steel porous / rough	$32 - 38$ / $4 - 29$	$78 - 100$ / $39 - 180$	$26 - 34$ / –	$3 - 7$ / –

Table 2. Variation of surface roughness parameters R_z and RP_c, porosity Φ and average pore diameter d_{pore} to compare the drop impact onto rough and porous surfaces. Note that from clarity reasons all the numbers have been rounded to integers.

and diameter $D = 2.4\,mm$ of the distilled water droplets are the same in both cases, but the target surfaces have different morphology. The regular groove structure can be clearly seen. In contrast to splash on unstructured targets, splashing on structured targets can look very different. For the target shown in the bottom series of Figure 4 prompt splash, like depicted in Figure 3, can be observed when the ejection of small droplets starts perpendicular to the groove pattern. By increasing drop impact velocity the lamella starts to detach from the surface perpendicular to the grooves direction. After detaching from the surface the lamella breaks up into a large number of secondary droplets. The drop ejection starts at the edge of the lamella. Parallel to the grooves stable rivulets are developed and no splashing is observed. Spreading is favoured parallel to the grooves.

The top row of Figure 4 shows a more developed version of lamella detachment on a structured target with higher roughness. The subsequent breakup of the lamella edge can be seen in the last two images. This type of "roughness corona splash" was also observed on unstructured targets, when obstacles initiate the detachment of the lamella from the substrate.

The lifted lamella on regularly grooved targets is also observed by [7]. The phenomenon looks similar to

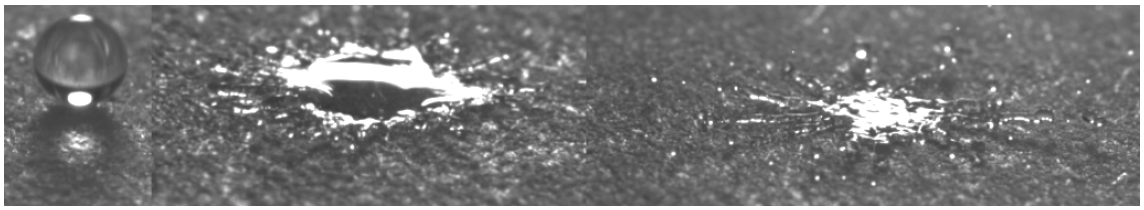

Figure 3. Prompt splash of a distilled water drop on a unstructured rough polyethylene surface (drop diameter: $D = 2.4\,mm$, impact velocity: $U = 3.1\,m/s$, $R_z = 117.7\,\mu m$, $RP_c = 27\,peaks/cm$).

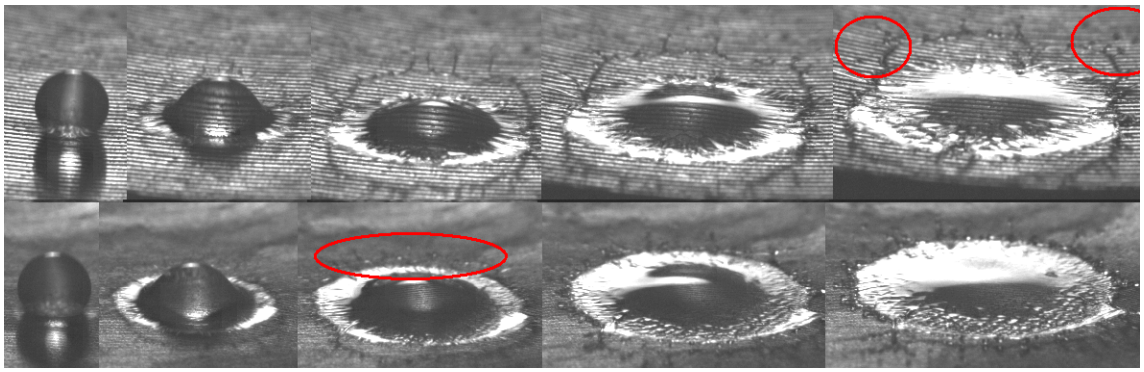

Figure 4. Observed splash mechanisms of impacting distilled water droplets onto structured bronze targets. Top series: Roughness corona splash ($R_z = 40.7\,\mu m$, $RP_c = 32.8\,peaks/cm$); Bottom series: Prompt splash and less distinct roughness corona splash ($R_z = 22.3\,\mu m$, $RP_c = 84\,peaks/cm$). Both impacts are characterized by drop diameter $D = 2.4\,mm$ and impact velocity $U = 4.3\,m/s$. Regions of prompt splash and lamella breakup are marked with a circle.

the phenomenon denoted as corona splash in literature. Referring to [4] corona splash on smooth surfaces is triggered by the pressure of the surrounding gas. However, the mechanism on the structured rough targets within the presented study is different. The grooves of the regular pattern act like a ramp to the lamella. Because the lamella has a momentum in vertical direction away from the surface, due to deflection by the "ramp", it detaches from the surface.

Similarities can be seen, when three different cases of corona splash are compared resulting after impact of a single drop onto a liquid film, onto a smooth dry rigid substrate and onto a rough target. In all three cases spreading film is deflected by a resistance of either outer liquid film [10], gas [4] or solid.

Corona splash was observed in experiments with isopropanol on targets with low roughness. A sequence of images is shown in Figure 5. [5] suggests splashing on a rough target to be a result of prompt splash and corona splash. By changing the impact velocity, the roughness of the surface or the fluid either prompt splash or corona splash will be more dominant. In Figure 5 the roughness has only a minor influence on the splash process and corona splash is observed. Because the phenomena of prompt and corona splash are linked on rough surfaces, a threshold between the two can not be easily defined.

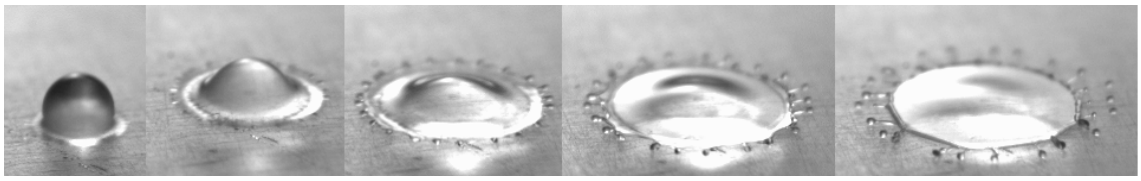

Figure 5. Corona splash of an isopropanol drop (drop diameter $D = 1.7\,mm$, impact velocity $U = 2.21\,m/s$) impacting onto the rough glass target ($R_z = 2.7\,\mu m$, $RP_c = 207.5\,peaks/cm$).

Splashing threshold on rough and porous targets

The roughness induced lamella detachment can be described accounting for the product of the vertical and the horizontal roughness measure $R_z \cdot RP_c$ which is a dimensionless measure of slope of the roughness elements. For a structured surface it describes how many ramps of equal height and width are disturbing the expanding lamella. For an unstructured target the ramp geometry is not uniform, but statistically averaged. The steeper the slope of the ramp the more the lamella is disturbed during its advance. This can be influenced either by increasing the number of peaks and variation of RP_c, or by increasing height of the roughness profile, which is covered by R_z. By decreasing both parameters one ends up in a smooth surface. However, for small values of $R_z \cdot RP_c$ the splash mechanism is supposed to change from prompt splash to corona splash as mentioned above.

Figure 6 a) shows the obtained splash threshold value of the Weber number, We_S, as a function of $R_z \cdot RP_c$ for the rough surfaces. It is noticeable that nearly all structured targets fall onto the correlated line, whereas the deviations for the unstructured targets are larger compared to the ones of the structured surfaces. The threshold for

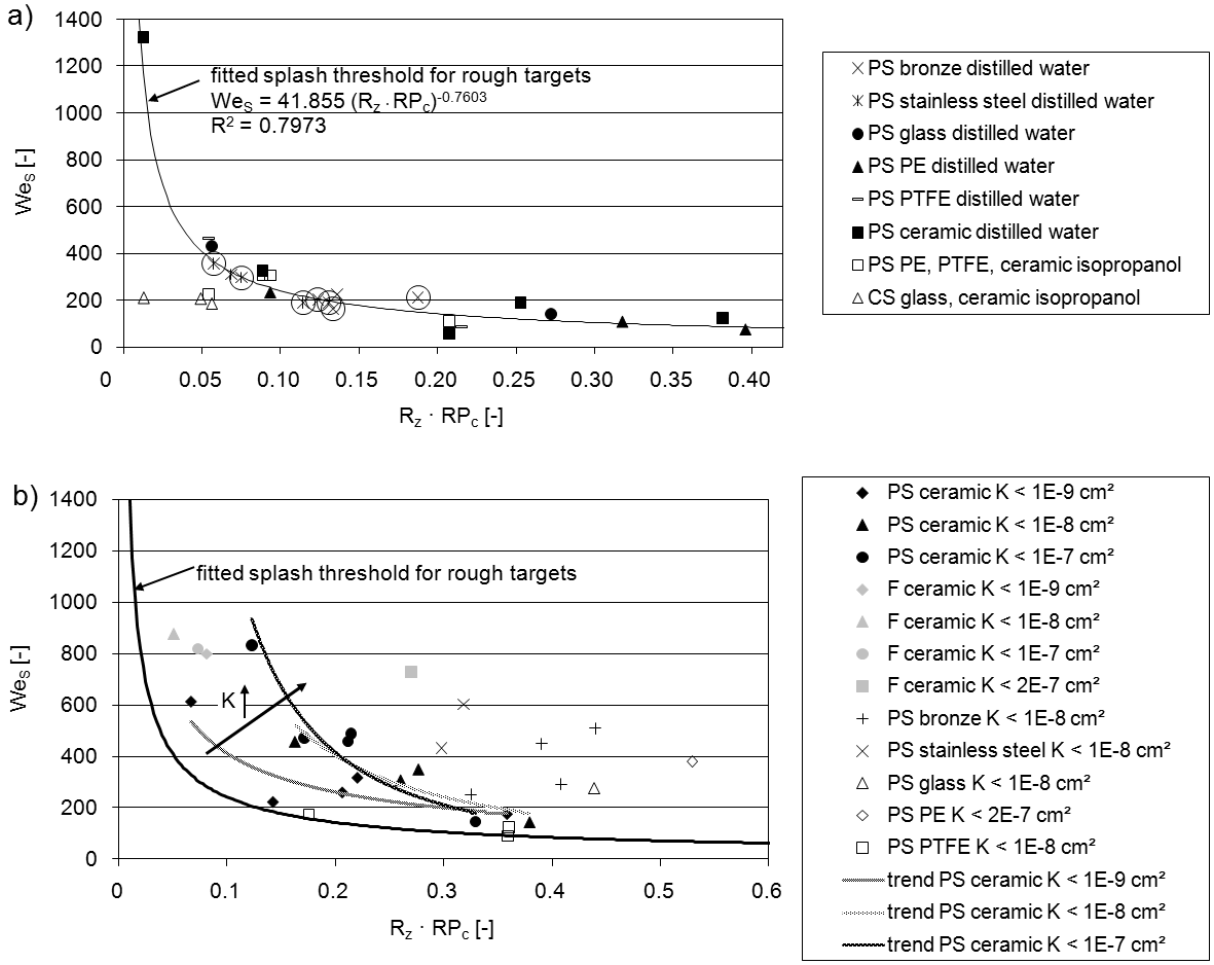

Figure 6. a) Weber number for the splashing threshold We_S on rough targets versus product of roughness amplitude R_z and number of roughness peaks per cm RP_c. Structured targets are additionally marked by ◯. PS means prompt splash, CS corona splash. b) Weber number for the distilled water splashing threshold We_S on porous targets versus product of roughness amplitude R_z and number of roughness peaks per cm RP_c. The trend for increasing permeability K is shown for the ceramic targets. For some targets no splash event has been measured and the largest Weber number (phenomenon is fingering (F)) is shown instead.

lamella detachment and fragmentation, resulting in prompt splash, can be described by a single line:

$$We_S = 41.855(R_z \cdot RP_c)^{-0.7603}. \tag{1}$$

Splashing threshold on rough surfaces is independent of the target material and wettability. The process is dominated by inertia rather than by capillary forces, which is also expressed in the definition of the We number.

The prompt splash threshold of isopropanol falls into the range of the prompt splash threshold of distilled water. It is concluded that viscosity plays a minor role for the two fluids investigated. Figure 6 a) also shows a transition region from prompt to corona splash for isopropanol drop impacts. The corona splash threshold is constant ($We_S \approx 200$) and the change of splash mechanism is observed for values of $R_z \cdot RP_c \approx 0.055$.

Contrary to this the distilled water splashing threshold on porous targets is found to be equal or higher for all investigated targets compared to the rough targets. Results are shown in Figure 6 b). On the one hand the splashing threshold of the porous PTFE targets can be described by the fitted line for the rough targets. On the other hand Eq. (1) can describe the splash threshold of the bronze, stainless steel, PE, glass and the most ceramic targets by no means.

Several parameters may be considered to explain the data arrangement of which all need further investigation:

- Important information of the roughness profile can get lost during the statistical evaluation, e.g. it is not distinguished between R_z being the result of a peak or a pore on the target surface.

- The static advancing contact angle on a smooth surface Θ_{adv} was measured to 133° for PTFE and 19° for ceramic. A large advancing contact angle will hinder the penetration of liquid into the pores to a larger extend than a small advancing contact angle.

- The suppression of splash on porous targets can be caused by liquid penetration due to high porosity and large pore size. By decreasing the volume of the expanding droplet, the impact We number is also decreased. Further kinetic energy is removed from the expanding lamella and dissipated within the porous structure.

The large number of investigated porous ceramic targets makes it possible to conduct a first approach considering the target permeability K which combines target porosity and pore size. K has been estimated by equating the following equation, which is published by [11],

$$K = \frac{\Phi}{8 \cdot n^2} \sum_{i=1}^{n} (2n-1) r_i^2 \, [cm^2] \tag{2}$$

with r_i in cm being the radius of class i of the pore size distribution, n the number of classes of the pore size distribution and Φ the porosity. The equation predicts the permeability for isotropic sands and natural stones in the range of $2.7 \cdot 10^{-11}\, cm^2 < K < 1.3 \cdot 10^{-6}\, cm^2$. For the samples presented within this study only the mean diameter of the pores d_{pore} is known. However, for a first analysis Eq. (2) is equated for $n = 1$ and d_{pore} and values of K range from $4.51 \cdot 10^{-11}\, cm^2$ to $1.19 \cdot 10^{-7}\, cm^2$.

Figure 6 b) shows four classes of K for the ceramic targets ($K < 10^{-9}$; $10^{-9} < K < 10^{-8}$; $10^{-8} < K < 10^{-7}$; $10^{-7} < K < 2 \times 10^{-7}$, cm^2). An increasing permeability tends to suppress the splash of an impacting droplet for the classified targets. For three classes curves indicate the trend of splash for a permeability class. It is worth to note merging of the curves for values of $R_z \cdot RP_c > 0.3$. This leads to the assumption of two counteracting mechanisms of which one promotes splash (increase in $R_z \cdot RP_c$) and one suppresses splash (increase in K).

Conclusion

Drop impact onto rough and porous surfaces was experimentally studied. Since the "conventional" expressions for splashing threshold known in the literature are not able to reliably describe our experimental data a new empirical correlation has been obtained.

Moreover, a first investigation of droplets splashing on porous targets has been presented. It was shown that the splashing threshold on porous surfaces significantly differs from the splashing threshold on rough surfaces. Further work is needed to explain these differences. Several parameters were considered of which roughness and permeability seem to be counteracting.

Acknowledgement

The authors would like to thank Kibriye Sercan, Jami Winzer, Dr. Ludwig Weiler and Emil Aulbach, who were involved in the manufacture of the porous ceramic targets at the Institute of Materials Science at the Technische Universität Darmstadt and Cécile Müller and Manuel Ludwig for their guidance during the roughness measurements at the Institute for Production Engineering and Forming Machines at the Technische Universität Darmstadt. A.L. acknowledges the financial support from the CSI, Darmstadt.

References

[1] Worthington, A. M., *Proc. R. Soc. London* 25:261-271 (1876).
[2] Rioboo, R., Tropea, C. and Marengo, M., *Atomiz. Sprays* 11:155-165 (2001).
[3] Vander Wal, R. L., Berger, G. M. and Mozes, S. D., *Exp. Fluids* 40:53-59 (2006).
[4] Xu, L., Zhang, W. W. and Nagel, S. R., *Phys. Rev. Lett.*, 94:184505 (2005).
[5] Xu, L., *Phys. Rev. E*, 75:056316 (2007).
[6] Mundo, C., Sommerfeld, M. and Tropea, C., *I. J. Multiphase Flow* 21:151-173 (1995).
[7] Range, K. and Feuillebois, F., *J. Colloid Interface Sci.* 203:16-30 (1998).
[8] Stow, C. D. and Hadfield, M. G., *Proc. R. Soc. London. A* 373:419-441 (1981).
[9] Trujillo, M. F., Mathews, W. S. and Peters, J. E., *I. J. Engine Research* 1:87-105 (2000).
[10] Yarin, A. L. and Weiss, D., *J. Fluid Mech.* 283:141-173 (1995).
[11] Marshall, T. J., *Journal of Soil Science* 9:1-8 (1958).